LAYOUT AND SIZE OPTIMIZATION OF TRUSSES WITH NATURAL FREQUENCY CONSTRAINTS USING IMPROVED RAY OPTIMIZATION ALGORITHM[*]

A. KAVEH[**] AND M. ILCHI GHAZAAN

Centre of Excellence for Fundamental Studies in Structural Engineering, Iran University of Science and Technology, Narmak, Tehran, P.O. Box 16846-13114, I. R. of Iran
Email: alikaveh@iust.ac.ir

Abstract– Natural frequency is one of the parameters that represent useful information about the dynamic behavior of structures. Controlling this parameter can decrease the probability of damage under dynamic loading. Weight optimization on layout and sizing with frequency constraints is a well known problem because of its highly non-linear behavior. Improved ray optimization (IRO) algorithm is utilized to solve truss layout and sizing optimization with multiple natural frequency constraints. This is a multi-agent algorithm and each agent is modeled as a ray of light with a location and direction. At each iteration, each light ray approaches a point which is defined based on the historically best position of the entire agents and the historically best positions of one agent to find the global or near-global optimum solution. To verify the efficiency of the IRO, five well-known benchmark problems are studied and their results illustrate the ability of the proposed algorithm in finding the optimal solution.

1. INTRODUCTION

In most of the low frequency vibration problems the response of a structure is a primary function of its fundamental frequency and mode shape [1]. This demonstrates that the natural frequencies of a structure should be controlled to keep the structural behavior desirable and avoid the resonance phenomenon.

Mass reduction conflicts with the frequency constraints, especially when they are lower bounded [2]. Also, frequency constraints are highly nonlinear, non-convex and implicit with respect to the design variables [1]. In this type of optimization problems which involves different design variables under complex constraints, local search algorithms are not suitable, and only global search algorithms should be used to obtain optimal solutions [3]. Therefore, mathematical programming approaches would be hard to apply and time-consuming in these optimization problems. Furthermore, a good starting point is vital for these methods to be executed successfully and they may converge to the local optima [4].

Meta-heuristics solve instances of problems that are believed to be hard in general, by exploring the usually large solution search space of these instances. These algorithms achieve this by reducing the effective size of the space and by exploring the search space efficiently. Moreover, mataheuristics are simple to design and easy to implement, and are very flexible. In recent years, these algorithms have been successfully applied to a large variety of structural optimization problems [5-10].

One recent addition to meta-heuristic methods is Ray Optimization (RO) [11] that is based on the transition of ray from one medium to another from physics. As the light passes through a surface of two

certain transparent materials, its path is changed slightly. This phenomenon was formulated by the Snell's law. In RO, by utilizing Snell's refraction law and a number of random terms, each agent moves in the search space to find the global or near-global optimum solution. Kaveh et al. [12] developed Improved Ray Optimization (IRO) and it is shown to be competent in structural optimization problems considering stresses and displacements as the constraints. The formulation of generating solution vectors and returning violated agents to feasible search space is changed in IRO. In this study, IRO is used to solve truss layout and sizing optimization with multiple natural frequency constraints.

The remaining sections of this paper are organized as follows. The proposed method is described in Section 2. The optimization design problem is formulated in Section 3. To show the efficiency and robustness of the IRO, it is applied to five well-known benchmark problems in Section 4. Finally the paper is concluded in Section 5.

2. IMPROVED RAY OPTIMIZATION ALGORITHM

Recently, a new physics-based optimization algorithm, so-called Ray Optimization (RO), is introduced by Kaveh and Khayatazad [11] that uses Snell's light refraction law. Similar to other multi-agent algorithms, RO has a number of agents, each agent being considered as a ray of light. When a light ray passes from a lighter medium to a darker medium, the direction of its movement is changed. Inspired by this phenomenon, RO is formulated to find a global or near-global optimum solution. To have a simple structure and more effective method, Improved Ray Optimization (IRO) algorithm was developed by [12]. The solution vectors are generated by new formulations and unlike the RO they have no limitation on the number of variables. Furthermore, the procedure which returns the violated agents into feasible search space is modified. In the following, the steps of the IRO algorithm are presented and for further clarity the corresponding pseudo code is provided in Fig. 1.

```
procedure Improved Ray Optimization (IRO)
        Initialize algorithm parameters
        for each agent
                Initial position and velocity are created randomly
                Fitness value is evaluated
        end for
        LBM and GB are updated          /* LBM and GB are local best memory and global best, respectively*/
        While maximum iterations is not fulfilled
                for each agent
                        new_position_i = current_position_i + movement_vector_i
                        Violated components are regenerated by Eq. (2)
                end for
                LBM and GB are updated
                for each agent
                        The direction of movement vector is calculated by Eq. (5)
                        The magnitude of movement vector is calculated by Eqs. (9-11)
                end for
        end while
end procedure
```

Fig. 1. Pseudo code of the Improved Ray Optimization algorithm

Step 1. The initial positions of the agents are determined randomly in the search space and the goal function is evaluated for each agent.

Step 2. A memory which saves some or all the best positions as local best memory (***LBM***) is considered, and the position of the best agent is saved as the global best (***GB***).

Step 3. The initial movement vectors of agents are stated as:

$$V_{ij} = -1 + 2.rand \qquad\qquad j=1,2,\ldots,n \tag{1}$$

where V_{ij} is the initial movement value of the jth variable for the ith agent. New positions are obtained by adding the position of each agent with its movement vector.

Step 4. If any component of an agent violates a boundary, it must be regenerated by the following formula:

$$X_{ij}^{k+1} = X_{ij}^{k} + 0.9(Int_{ij} - X_{ij}^{k}) \tag{2}$$

where X_{ij}^{k+1} and X_{ij}^{k} are the refined component and component of the jth variable for the ith agent in $(k+1)$th and kth iteration, respectively. Int_{ij} is the intersection point (in case an agent violates a boundary, it intersects the boundary at a specified point, because of having a specific movement vector). After regenerating all violated components, the goal function is evaluated for each agent and the LBM and GB are updated.

Step 5. Consider the origin as a point which each agent wants to move toward and is specified by

$$O_i^K = \frac{(ite + k).\boldsymbol{GB} + (ite - k).\boldsymbol{LB}}{2.ite} \tag{3}$$

where O_i^k is the origin of the ith agent for the kth iteration, and ite is the total number of iterations for the optimization process. For each agent, $\boldsymbol{LB}$ is a solution vector which is selected randomly from local best memory ($\boldsymbol{LBM}$). Target vector is defined as:

$$\boldsymbol{Tv}_i = O_i - X_i \tag{4}$$

where $\boldsymbol{Tv}_i$ and X_i are target vector and current position of the ith agent, respectively.

Step 6. Direction of the new movement vector is defined by

$$V_i^{k+1} = \alpha.Tv_i^{k} + \beta.V_i^{k} \tag{5}$$

$$\alpha = 1 + (\frac{k}{ite}) \tag{6}$$

$$\beta = 1 - 0.5(\frac{k}{ite}) \tag{7}$$

where V_i^{k+1} and V_i^{k} are movement vectors for the ith agent in $(k+1)$th iteration and kth iteration, respectively. Finally, all the V_i^{k+1} vectors should be normalized.

Step 7. Possibility like *Stoch* is considered and the magnitude of movement vectors are defined as:
a. with probability like *Stoch*,

$$V_{ij}^{k+1} = -1 + 2.rand \tag{8}$$

$$V_i^{K+1} = \frac{V_i^{k+1}}{norm(V_i^{k+1})} . \frac{a}{d} .rand \tag{9}$$

b. with probability like *(1–stoch)*,
If $norm(O_i^{k} - X_i^{k}) = 0$, then

$$V_i^{k+1} = \frac{V_i^k}{norm(V_i^k)} . rand . 0.001 \tag{10}$$

Otherwise,

$$V_i^{K+1} = V_i^{k+1} . \frac{a}{d} \tag{11}$$

$$a = \sqrt{\sum_{i=1}^{n} (X_{j,\max} - X_{j,\min})^2} \tag{12}$$

$$d = d + r.d.(\frac{k}{ite}) \tag{13}$$

where $X_{j,max}$ and $X_{j,min}$ are the upper and lower bounds for the *j*th design variable, respectively. *d* and *r* are constant factors.

The optimization process is terminated after a fixed number of iterations. If it is not fulfilled each movement vector is added to its current position vector and the process of optimization is continued from Step 4.

3. STATEMENT OF THE PROBLEM

In this study, the objective is to minimize the weight of the structure while satisfying some constraints on natural frequencies. The design variables are cross-sectional areas of structural elements and also, in some problems, several nodal coordinates are considered as variables. The mathematical formulation of these problems can be expressed as follows:

$$\text{Find} \qquad \{X\} = [x_1, x_2, ..., x_{ng}], \quad x_i \in D_i$$

$$\text{to minimize} \qquad W(\{X\}) = \sum_{i=1}^{nm} \rho_i A_i L_i \tag{14}$$

$$\text{subjected to:} \qquad g_j(\{X\}) \le 0, \quad j = 1, 2, ..., n$$

where $\{X\}$ is the set of design variables; *ng* is the number of optimization variables which depends on element grouping; D_i is the allowable set of values for the design variable x_i which can be considered either as a continuous set or as a discrete one; $W(\{X\})$ is the weight of the structure; *nm* is the number of members of the structure; ρ_i, A_i and L_i denotes the material density, cross-sectional area and the length of the *i*th member, respectively; $g_j(\{X\})$ denote design constraints; *n* is the number of the constraints.

In this study, the penalty function method is utilized as a constraint-handling approach, and the constrained objective function is expressed as follows:

$$f_{cost}(\{X\}) = (1 + \varepsilon_1 . \upsilon)^{\varepsilon_2} \times W(\{X\}), \quad \upsilon = \sum_{j=1}^{n} \max\left[0, g_j(\{X\})\right] \tag{15}$$

where *n* represents the number of evaluated constraints for each individual design, and υ is the total constraint violation. The constants ε_1 and ε_2 are selected considering the exploration and the exploitation rates of the search space. Here, ε_1 is set to unity and ε_2 starts from 1.5 and linearly increases to 3. These values penalize the unfeasible solutions more severely as the optimization process proceeds. As a result, in the early stages, the agents are free to explore the search space, but at the end they tend to choose solutions without violation.

4. BENCHMARK EXAMPLES

The five benchmark examples given in this section have been widely used to show the validity and effectiveness of the optimization algorithms. These examples are as follows:

- ➤ A 10-bar plane truss with ten sizing variables;
- ➤ A simply supported 37-bar plane truss with five layout variables and fourteen sizing variables;
- ➤ A 52-bar dome-like truss with five layout variables and eight sizing variables;
- ➤ A 72-bar space truss with sixteen sizing variables.
- ➤ A 120-bar dome truss with seven sizing variables.

In our simulations, the number of agents and **Stoch** are set to 20 and 0.35, respectively. In all the examples the values of *d* and *r* are considered as 10 and 5, respectively. Each example has been solved twenty times independently and the best results are reported here.

a) A 10-bar plane truss

The ten bar plane truss shown in Fig. 2, is a well-known benchmark problem in the field of weight optimization of the structures with frequency constraints. The cross-sectional area of each of the members is considered to be an independent variable. As can be seen in Fig. 2, at each free node (1–4) a non-structural mass of 453.6kg (1000lb) is attached. Material properties, variable bounds and frequency constraints are listed in Table 1. In this article, the allowable maximum area of the cross section is 50 cm^2.
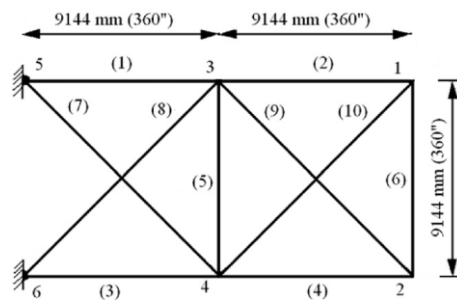

Fig. 2. A 10-bar truss

Table 1. Material properties, variable bounds and frequency constraints for the 10-bar truss

Property/unit	Value
E (Modulus of elasticity)/ N/m^2	6.895×10^{10}
ρ (Material density)/ kg/m^3	2767.99
Added mass/ kg	453.6
Allowable range for cross section/ m^2	$6.45\times10^{-5} \leq A \leq 0.005$
Constraints on first three frequencies/ Hz	$\omega_1 \geq 7$, $\omega_2 \geq 15$, $\omega_3 \geq 20$

This problem has been investigated by many authors using different optimization methods. Wang et al. [13] have employed an evolutionary node shift method and Lingyun et al. [14] have used a niche hybrid genetic algorithm to optimize this structure. Gomes [2] has studied this problem using the particle swarm algorithm. Miguel and Fadel Miguel [3] have utilized harmony search (HS) and Firefly Algorithm (FA) to optimize this example.

The optimum design, natural frequencies and statistical results are shown in Tables 2–4, respectively. As it can be observed in Table 2, the best answer is achieved using IRO, and all of the constraints are satisfied, as may be seen in Table 3. The statistical results of twenty independent runs presented in Table 4 demonstrates slight standard deviation from the mean value and shows that the algorithm is effective to solve the sizing optimization of this structure with multiple frequency constraints. Figure 3 illustrates the best and average convergence history for the results of the IRO algorithm. The best weights are obtained after 13,700 analyses and the average number of analysis for independent runs is 16,000 analyses.

Table 2. Optimal design cross sections (cm^2) for the ten bar planar truss

Element number	Wang et al. [13]	Lingyun et al. [14]	Gomes [2]	Miguel & Fadel Miguel [3]		Present work
				HS	FA	
1	32.456	42.23	37.712	34.282	36.198	35.0472
2	16.577	18.555	9.959	15.653	14.030	15.1375
3	32.456	38.851	40.265	37.641	34.754	35.8134
4	16.577	11.222	16.788	16.058	14.900	15.0711
5	2.115	4.783	11.576	1.069	0.654	0.6450
6	4.467	4.451	3.955	4.740	4.672	4.6301
7	22.810	21.049	25.308	22.505	23.467	23.9399
8	22.810	20.949	21.613	24.603	25.508	23.8225
9	17.490	10.257	11.576	12.867	12.707	12.5297
10	17.490	14.342	11.186	12.099	12.351	12.9266
Weight (kg)	553.8	542.75	537.98	534.99	531.28	531.24

Table 3. Optimum design of natural frequencies (Hz) for the 10-bar truss

Frequency number	Wang et al. [13]	Lingyun et al. [14]	Gomes [2]	Miguel & Fadel Miguel [3]		Present work
				HS	FA	
1	7.011	7.008	7.000	7.0028	7.0002	7.0013
2	17.302	18.148	17.786	16.7429	16.1640	16.1770
3	20.001	20.000	20.000	20.0548	20.0029	20.0150
4	20.100	20.508	20.063	20.3351	20.0221	20.0420
5	30.869	27.797	27.776	28.5232	28.5428	28.5808
6	32.666	31.281	30.939	29.2911	28.9220	29.1402
7	48.282	48.304	47.297	49.0342	48.3538	48.6016
8	52.306	53.306	52.286	51.7451	50.8004	51.1780

Table 4. Statistical results for the 10-bar truss

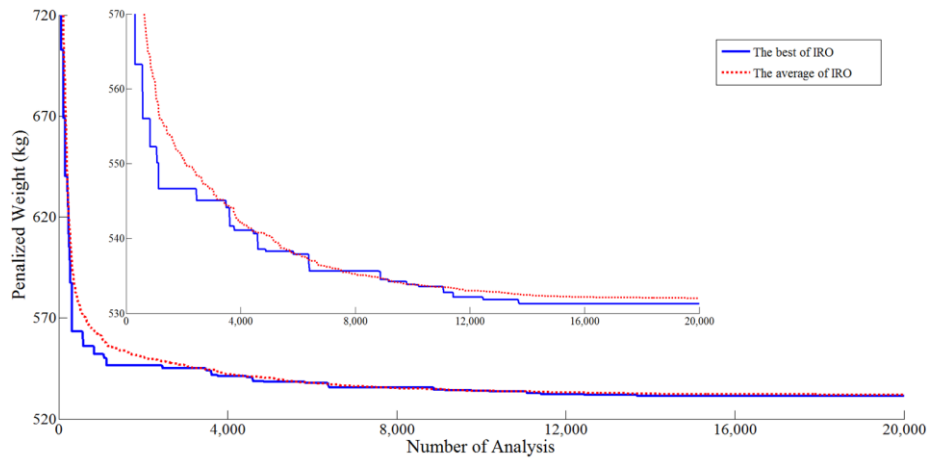| Mean Weight using IRO (kg)	Standard deviation (kg)	Number of searches
532.00	1.43	16000

Fig. 3. The convergence curves for the 10-bar truss

b) *A simply supported 37-bar plane truss*

The simply supported 37-bar plane truss with initial configuration shown in Fig. 4 is considered as the second standard test problem. Non-structural mass of 10kg is attached at each of the free nodes on the lower chord which remain fixed during the design process as can be seen in Fig. 4.
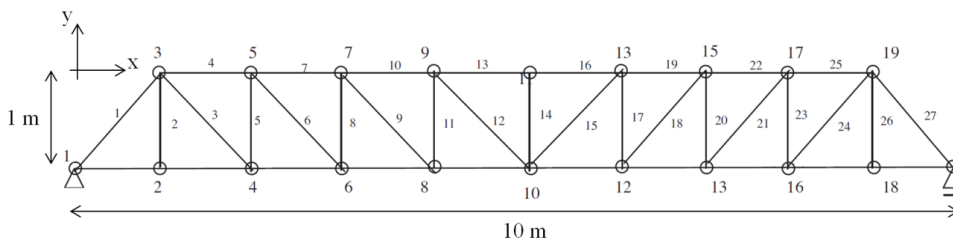

Fig. 4. A simply supported 37-bar planar truss

Nodal coordinates in the upper chord and member areas are regarded as design variables. All members on the lower chord (numbers 28–37) are modeled as bar elements with constant rectangular cross sectional areas of 4×10^{-3} m^2 and the others are modeled as bar elements with initial cross-sectional areas of 1×10^{-4} m^2. In the optimization process, nodes of the upper chord can be shifted vertically. In addition, nodal coordinates and member areas are linked to maintain the structural symmetry. Thus, only five layout variables and fourteen sizing variables will be redesigned for the optimization. Table 5 shows the material properties, frequency constraints and added masses for this example.

Table 5. Material properties, frequency constrains and added masses for 37-bar truss

Property/unit	Value
E (Modulus of elasticity)/ N/m^2	2.1×10^{11}
ρ (Material density)/ kg/m^3	7800
Added mass/ kg	10
Constraints on first three frequencies/ Hz	$\omega_1 \geq 20$, $\omega_2 \geq 40$, $\omega_3 \geq 60$

This example has been studied by Wang et al. [13], Lingyun et al. [14], Gomes [2], Kaveh and Zolghadr [4], Miguel and Fadel Miguel [3]. Table 6 summarizes the optimal results obtained by different researchers. The proposed algorithm has obtained a structure which is slightly lighter than the structure obtained by other methods. Natural frequencies and statistical results are shown in Tables 7-8, respectively. None of the frequency constraints were violated. Figure 5 shows the 37-bar truss optimized by the IRO.

Table 6. Final cross-sectional areas and node coordinates for the 37-bar simply supported planar truss

Variables	Wang et al. [13]	Lingyun et al. [14]	Gomes [2]	Kaveh & Zolghadr [4]		Miguel & Fadel Miguel [3]		Present work
				CSS	Enhanced CSS	HS	FA	
Y_3 , Y_{19} (m)	1.2086	1.1998	0.9637	0.8726	1.0289	0.8415	0.9392	0.9641
Y_5 , Y_{17} (m)	1.5788	1.6553	1.3978	1.2129	1.3868	1.2409	1.3270	1.3490
Y_7 , Y_{15} (m)	1.6719	1.9652	1.5929	1.3826	1.5893	1.4464	1.5063	1.5422
Y_9 , Y_{13} (m)	1.7703	2.0737	1.8812	1.4706	1.6405	1.5334	1.6086	1.6719
Y_{11} (m)	1.8502	2.3050	2.0856	1.5683	1.6835	1.5971	1.6679	1.7466
A_1 , A_{27} (cm^2)	3.2508	2.8932	2.6797	2.9082	3.4484	3.2031	2.9838	2.9082
A_2 , A_{26} (cm^2)	1.2364	1.1201	1.1568	1.0212	1.5045	1.1107	1.1098	1.0494
A_3 , A_{24} (cm^2)	1.0000	1.0000	2.3476	1.0363	1.0039	1.1871	1.0091	1.0020
A_4 , A_{25} (cm^2)	2.5386	1.8655	1.7182	3.9147	2.5533	3.3281	2.5955	2.6153
A_5 , A_{23} (cm^2)	1.3714	1.5962	1.2751	1.0025	1.0868	1.4057	1.2610	1.0915
A_6 , A_{21} (cm^2)	1.3681	1.2642	1.4819	1.2167	1.3382	1.0883	1.1975	1.2766
A_7 , A_{22} (cm^2)	2.4290	1.8254	4.6850	2.7146	3.1626	2.1881	2.4264	2.7346
A_8 , A_{20} (cm^2)	1.6522	2.0009	1.1246	1.2663	2.2664	1.2223	1.3588	1.4154
A_9 , A_{18} (cm^2)	1.8257	1.9526	2.1214	1.8006	1.2668	1.7033	1.4771	1.5225
A_{10} , A_{19} (cm^2)	2.3022	1.9705	3.8600	4.0274	1.7518	3.1885	2.5648	2.2575
A_{11} , A_{17} (cm^2)	1.3103	1.8294	2.9817	1.3364	2.7789	1.0100	1.1295	1.3206
A_{12} , A_{15} (cm^2)	1.4067	1.2358	1.2021	1.0548	1.4209	1.4074	1.3199	1.2462
A_{13} , A_{16} (cm^2)	2.1896	1.4049	1.2563	2.8116	1.0100	2.8499	2.9217	2.3298
A_{14} (cm^2)	1.0000	1.0000	3.3276	1.1702	2.2919	1.0269	1.0004	1.0000
Weight (kg)	366.5	368.84	377.20	362.84	362.38	361.50	360.05	359.97

Table 7. Natural frequencies (Hz) obtained by various methods for the 37-bar simply supported planar truss

Frequency number	Wang et al. [13]	Lingyun et al. [14]	Gomes [2]	Kaveh & Zolghadr [4]		Miguel & Fadel Miguel [3]		Present work
				CSS	Enhanced CSS	HS	FA	
1	20.0850	20.0013	20.0001	20.0000	20.0028	20.0037	20.0024	20.0004
2	42.0743	40.0305	40.0003	40.0693	40.0155	40.0050	40.0019	40.0351
3	62.9383	60.0000	60.0000	60.6982	61.2798	60.0082	60.0043	60.0013
4	74.4539	73.0444	73.0440	75.7339	78.1100	77.9753	77.2153	76.3818
5	90.0576	89.8244	89.8240	97.6137	98.4100	99.2564	96.9900	96.7195

Table 8. Statistical results for the 37-bar space truss

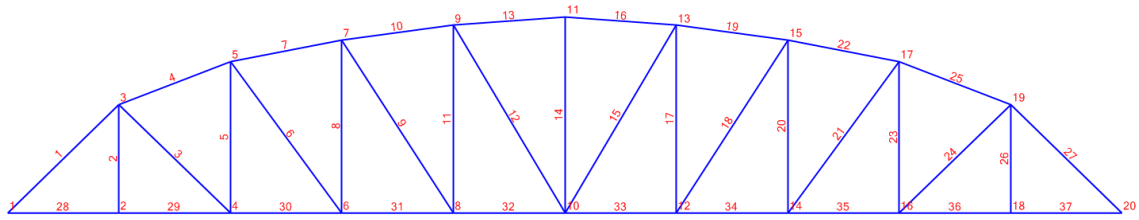| Mean Weight using IRO (kg)	Standard deviation (kg)	Number of searches
360.85	0.78	18000

Fig. 5. Final configuration design optimized by the present paper using IRO

c) A 52-bar dome-like truss

The third benchmark problem is the 52-bar dome-like truss with initial configuration depicted in Figs. 6 and 7. Non-structural masses of 50kg are attached to all the free nodes. Material properties, frequency constraints and variable bounds for this example are summarized in Table 9. All the elements of the structure are categorized in eight groups according to Table 10 and the section area of each bar is initially equal to 2×10^{-4} m^2. All free nodes are permitted to move in a symmetrical manner, by the amount ±2m in each allowable direction from their initial position. Thus there are 13 independent design variables, being five layout and eight sizing variables.
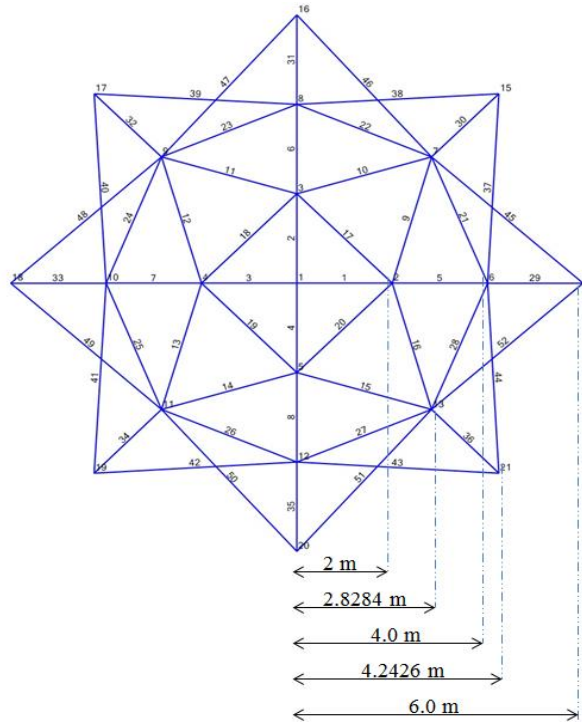

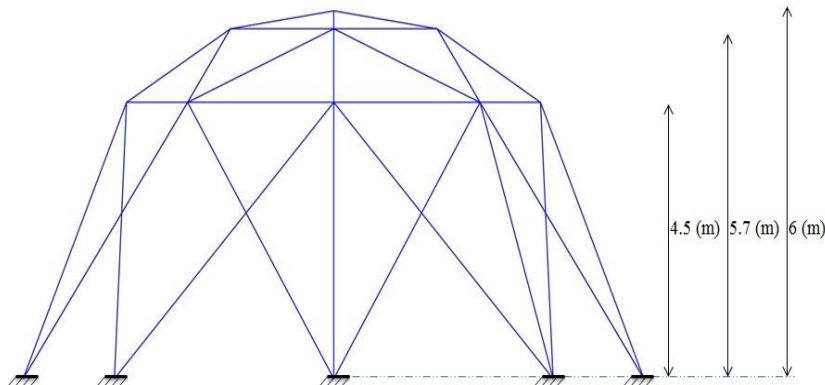Fig. 6. Initial configuration design for the dome structure (top view)

Fig. 7. Initial configuration design for the dome structure (lateral view)

Table 9. Material properties, frequency constraints and variable bounds for the 52-bar space truss

Property/unit	Value
E (Modulus of elasticity)/ N/m^2	2.1×10^{11}
ρ (Material density)/ kg/m^3	7800
Added mass/ kg	50
Allowable range for cross section/ m^2	$0.0001 \leq A \leq 0.001$
Constraints on frequencies/ Hz	$\omega_1 \leq 15.9155$, $\omega_2 \geq 28.6479$

Table 10. Element grouping for the 52-bar space truss

Group number	Elements
1	1-4
2	5-8
3	9-16
4	17-20
5	21-28
6	29-36
7	37-44
8	45-52

This problem has also been studied by Lingyun et al. [14] using niche hybrid genetic algorithm (NHGA), and Gomes [2] using particle swarm optimization algorithm (PSO). Kaveh and Zolghadr [15] have analyzed the problem using the hybridized CSS–BBBC with a trap recognition capability. Miguel and Fadel Miguel [3] have used HS and FA to optimize this example.

Table 11 shows that IRO yields the least weight for this problem, which is 195.38kg; furthermore, all of the constraints are satisfied according to Table 12. Statistical results are reported in Table 13. Figure 8 represents the optimized layout of the 52 bar dome-like truss obtained by IRO.

Table 11. Cross-sectional areas and node coordinates obtained by different researchers (the 52-bar space truss)

Variables	Lingyun et al. [14]	Gomes [2]	Kaveh & Zolghadr [15] CSS	Kaveh & Zolghadr [15] CSS-BBBC	Miguel & Fadel Miguel [3] HS	Miguel & Fadel Miguel [3] FA	Present work
Z_1 (m)	5.8851	5.5344	4.000	5.331	4.7374	6.4332	5.7600
X_2 (m)	1.7623	2.0885	1.955	2.134	1.5643	2.2208	2.1959
Z_2 (m)	4.4091	3.9283	3.742	3.719	3.7413	3.9202	3.7150
X_6 (m)	3.4406	4.0255	3.841	3.935	3.4882	4.0296	3.9269
Z_6 (m)	3.1874	2.4575	2.500	2.500	2.6274	2.5200	2.5000
A_1 (cm^2)	1.0004	0.3696	1.0000	1.0000	1.0085	1.0050	1.0000
A_2 (cm^2)	2.1417	4.1912	1.0000	1.3056	1.4999	1.3823	1.1889
A_3 (cm^2)	1.4858	1.5123	2.3858	1.4230	1.3948	1.2295	1.2411
A_4 (cm^2)	1.4018	1.5620	1.0000	1.3851	1.3462	1.2662	1.4422
A_5 (cm^2)	1.9116	1.9154	1.4659	1.4226	1.6776	1.4478	1.3932
A_6 (cm^2)	1.0109	1.1315	1.0000	1.0000	1.3704	1.0000	1.0000
A_7 (cm^2)	1.4693	1.8233	2.9158	1.5562	1.4137	1.5728	1.6929
A_8 (cm^2)	2.1411	1.0904	1.0000	1.4485	1.9378	1.4153	1.3569
Weight (kg)	236.05	228.38	235.931	197.309	214.94	197.53	195.38

Table 12. Natural frequencies (Hz) obtained by various methods (the 52-bar space truss)

Frequency number	Lingyun et al. [14]	Gomes [2]	Kaveh & Zolghadr [15] CSS	Kaveh & Zolghadr [15] CSS-BBBC	Miguel & Fadel Miguel [3] HS	Miguel & Fadel Miguel [3] FA	Present work
1	12.8051	12.751	14.984	12.987	12.2222	11.3119	11.4437
2	28.6489	28.649	28.649	28.648	28.657	28.6529	28.6529
3	28.6489	28.649	28.672	28.679	28.65	28.6529	28.7014
4	29.5398	28.803	28.7228	28.713	28.661	28.8030	28.7179
5	30.2443	29.230	29.3432	30.262	30.0997	28.8030	29.1276

Table 13. Statistical results for the 52-bar space truss

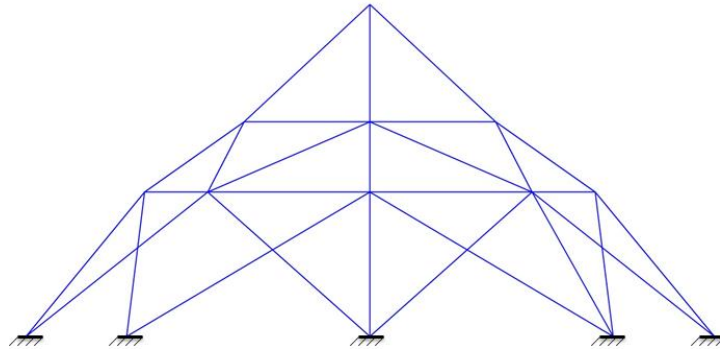| Mean Weight using IRO (kg)	Standard deviation (kg)	Number of searches
196.43	1.81	17000

Fig. 8. The optimized layout of the 52-bar dome-like space truss using IRO

d) A 72-bar space truss

The 72-bar space truss shown in Fig. 9 is the third benchmark example. The pre-defined layout of the structure remains unchanged during the optimization process, thus the design variables are the member cross sectional areas, treated as continuous design variables. These variables are classified in 16 design groups according to Table 14. Four non-structural masses of 2268 kg are attached to the nodes 1 through 4. Material properties, variable bounds, frequency constraints and added masses are listed in Table 15. In the optimization process two cases are considered. In the first case, the upper bound of the cross section is taken as 2×10^{-3} m^2 and in the second case it is 5×10^{-3} m^2.
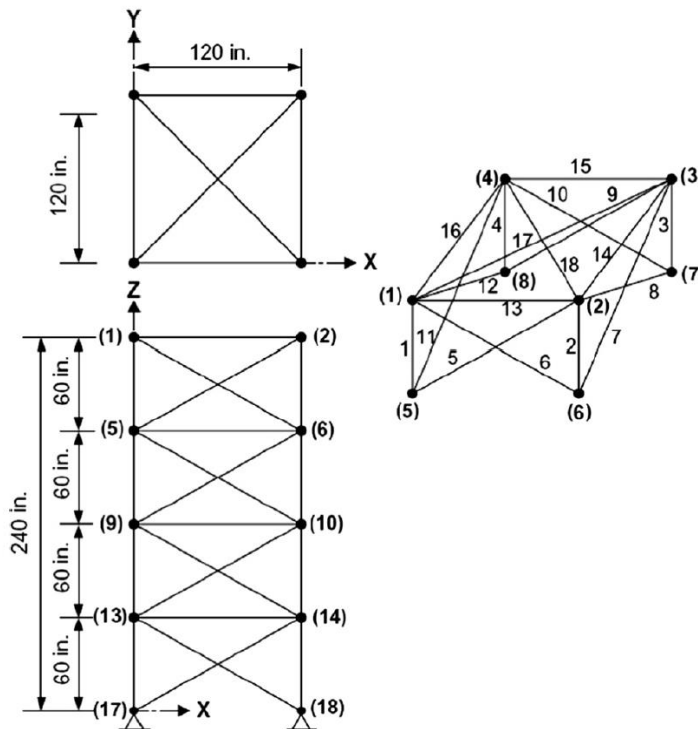

Fig. 9. A 72-bar space truss

This problem has also been studied by Gomes [2], Kaveh and Zolghadr [4], Miguel and Fadel Miguel [3]. The optimum design, natural frequencies and statistical results are shown in Tables 16-18, respectively. The IRO algorithm can find the best design among the other methods which is 327.597kg and none of the frequency constraints are violated. While the search space is expanded in case 2, the proposed method can achieve the structure which is approximately equal to the best one found. Figure 10 represents the convergence curves of the best results obtained by the proposed algorithm.

Table 14. Element grouping the 72-bar space truss

Group number	Elements
1	1-4
2	5-12
3	13-16
4	17-18
5	19-22
6	23-30
7	31-34
8	35-36
9	37-40
10	41-48
11	49-52
12	53-54
13	55-58
14	59-66
15	67-70
16	71-72

Table 15. Material properties, frequency constrains and added mass for the 72-bar space truss

Property/unit	Value
E (modulus of elasticity)/ N/m^2	6.895×10^{10}
ρ (Material density)/ kg/m^3	2767.99
Added mass/ kg	2268
Design variable lower bound/ m^2	0.645×10^{-4}
Constraints on frequencies/ Hz	$\omega_1 = 4$, $\omega_3 \geq 6$

Table 16. Optimal design cross sections (cm^2) for the 72-bar space truss from various methods

Design variable	Gomes [2]	Kaveh & Zolghadr [4]		Miguel & Fadel Miguel [3]		Present work	
		CSS	Enhanced CSS	HS	FA	Case 1	Case 2
1	2.987	2.528	2.252	3.6803	3.3411	3.5414	3.5659
2	7.849	8.704	9.109	7.6808	7.7587	7.9305	7.9281
3	0.645	0.465	0.648	0.6450	0.6450	0.6450	0.6450
4	0.645	0.645	0.645	0.6450	0.6450	0.6450	0.6450
5	8.765	8.283	7.946	9.4955	9.0202	7.9751	8.0244
6	8.153	7.888	7.703	8.2870	8.2567	8.0034	8.0081
7	0.645	0.645	0.647	0.6450	0.6450	0.6450	0.6450
8	0.645	0.645	0.646	0.6461	0.6450	0.6450	0.6450
9	13.450	14.666	13.465	11.4510	12.0450	12.9353	12.7370
10	8.073	6.793	8.250	7.8990	8.0401	8.0249	8.0637
11	0.645	0.645	0.645	0.6473	0.6450	0.6450	0.6450
12	0.645	0.645	0.646	0.6450	0.6450	0.6450	0.6450
13	16.684	16.464	18.368	17.4060	17.3800	17.2134	17.3488
14	8.159	8.809	7.053	8.2736	8.0561	8.1675	8.1273
15	0.645	0.645	0.645	0.6450	0.6450	0.6450	0.6450
16	0.645	0.645	0.646	0.6450	0.6450	0.6450	0.6450
Weight (kg)	328.823	328.814	328.393	328.334	327.691	327.597	327.622

Table 17. Natural frequencies (Hz) obtained by various methods for the 72-bar space truss

Frequency number	Gomes [2]	Kaveh & Zolghadr [4]		Miguel & Fadel Miguel [3]		Present work	
		CSS	Enhanced CSS	HS	FA	Case 1	Case 2
1	4.000	4.000	4.000	4.0000	4.0000	4.000	4.000
2	4.000	4.000	4.000	4.0000	4.0000	4.000	4.000
3	6.000	6.006	6.004	6.0000	6.0000	6.000	6.000
4	6.219	6.210	6.155	6.2723	6.2468	6.245	6.246
5	8.976	8.684	8.390	9.0749	9.0380	9.075	9.078

Table 18. Statistical results for the 72-bar space truss

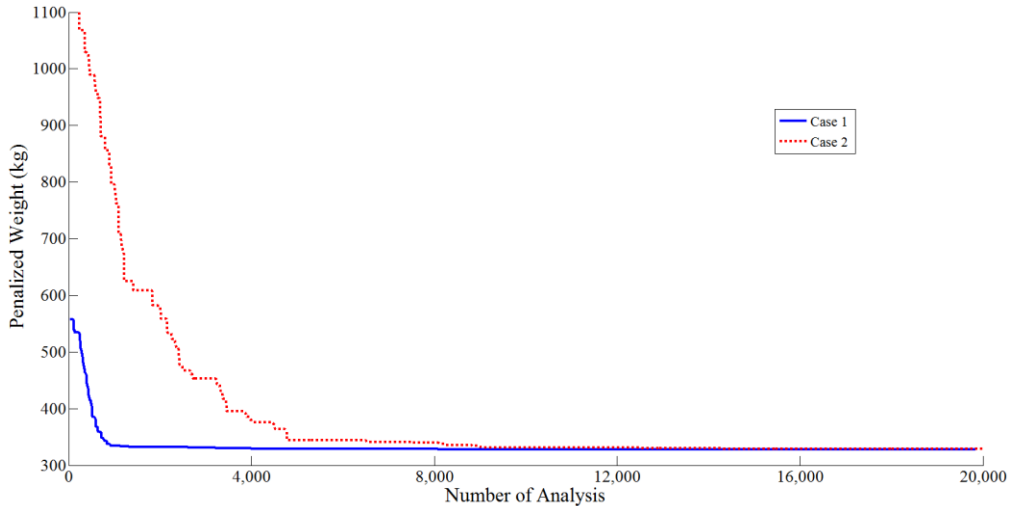| Case	Mean Weight using IRO (kg)	Standard deviation (kg)	Number of searches
1	328.19	2.07	16000
2	329.80	2.24	17000

Fig. 10. The convergence curves for the 72-bar space truss

e) A 120-bar dome truss

The 120-bar dom*e truss is shown in Fig. 11 and it is addressed as a size optimization problem with frequency constraints [15]. Non-structural masses are attached to all free nodes as follows: 3000 kg at node one, 500kg at nodes 2–13 and 100kg at the remaining nodes. Material properties, frequency constraints and variable bounds for this example are summarized in Table 19. The 120 members are categorized into seven groups, because of symmetry.
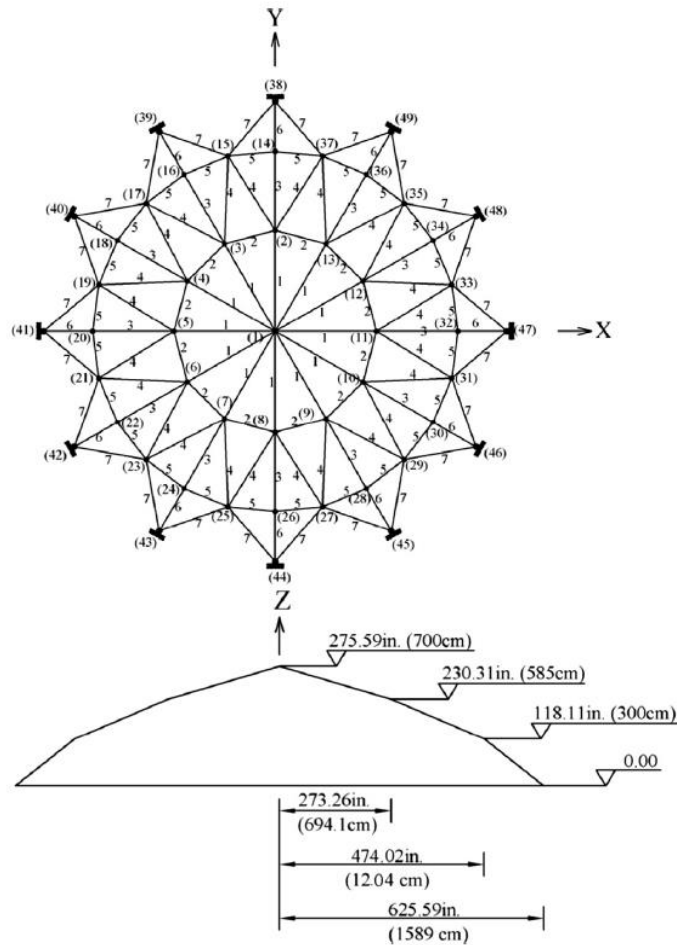

Fig. 11. The 120-bar dome truss

Table 19. Material properties, frequency constraints and variable bounds for the 120-bar dome truss

Property/unit	Value
E (Modulus of elasticity)/ N/m^2	2.1×10^{11}
ρ (Material density)/ kg/m^3	7971.810
Allowable range for cross section/ m^2	$0.0001 \leq A \leq 0.01293$
Constraints on frequencies/ Hz	$\omega_1 \geq 9$, $\omega_2 \geq 11$

Table 20 demonstrates the design variables results and the final weight for the optimized truss. It should be noted that good results were obtained with the IRO algorithm. Table 21 shows the optimized structural frequencies (Hz) for various methods. None of the frequency constraints were violated. The statistical results for twenty independent runs are listed in Table 22. Figure 12 shows the best and average of twenty runs convergence history for the proposed algorithm.

Table 20. Optimal design cross sections (cm^2) for the 120-bar dome truss

Design variable	Kaveh & Zolghadr [15]		Present work
	CSS	CSS-BBBC	
1	21.710	17.478	19.7332
2	40.862	49.076	40.5101
3	9.048	12.365	11.5088
4	19.673	21.979	21.8446
5	8.336	11.190	9.9880
6	16.120	12.590	12.6098
7	18.976	13.585	14.6800
Weight (kg)	9204.51	9046.34	8895.42

Table 21. Natural frequencies (Hz) obtained by various methods for the 120-bar dome truss

Frequency number	Kaveh & Zolghadr [15]		Present work
	CSS	CSS-BBBC	
1	9.002	9.000	9.000
2	11.002	11.007	11.001
3	11.006	11.018	11.002
4	11.015	11.026	11.011
5	11.045	11.048	11.051

Table 22. Statistical results for the 120-bar dome truss

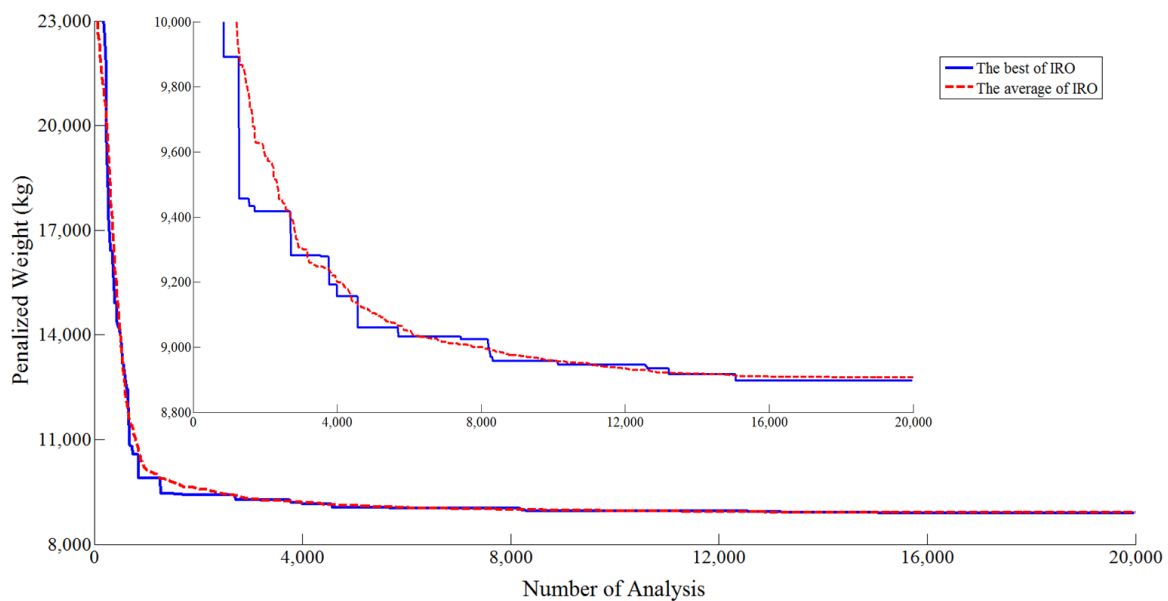| Mean Weight using IRO (kg)	Standard deviation (kg)	Number of searches
8905.21	4.92	16300

Fig. 12. The convergence curves for the 120-bar dome truss

5. CONCLUDING REMARKS

In this paper, layout and size optimization of truss structures with frequency constraints is investigated. This is a highly non-linear and non-convex optimization problem with several local optima because of the different nature of the variables involved, their different order and the sensitivity of the natural frequencies to layout modifications.

To verify the performance of the IRO, five well-known benchmark problems are studied and their results are compared to those of some other methods. Comparisons show that the proposed algorithm has obtained the best results for all of the numerical examples. It performed well in terms of accuracy and the number of objective function evaluations. Therefore, the IRO algorithm can be considered as an acceptable stochastic search technique for layout and sizing optimization of trusses with multiple natural frequency constraints.

REFERENCES

1. Grandhi, R. V. (1993). Structural optimization with frequency constraints-a review. *AIAA Journal*, Vol. 31, No. 12, pp. 2296–2303.

2. Gomes, M. H. (2011). Truss optimization with dynamic constraints using a particle swarm algorithm. *Expert Systems and Applications*, Vol. 38, No. 1, pp. 957–968.

3. Miguel, L. F. F. & Fadel Miguel L. F. (2012). Shape and size optimization of truss structures considering dynamic constraints through modern meta-heuristic algorithms. *Expert Systems and Applications*, Vol. 39, pp. 9458-9467.

4. Kaveh, A. & Zolghadr, A. (2011). Shape and size optimization of truss structures with frequency constraints using enhanced charged system search algorithm. *Asian Journal of Civil Engineering*, Vol. 12, No. 4, pp. 487-509.

5. Hasançebi, O., Carbas, S., Doǧan, E., Erdal, F. & Saka, M.P. (2009). Performance evaluation of metaheuristic search techniques in the optimum design of real size pin jointed structures. *Computers and Structures*, Vol. 87, No. 5–6, pp. 284–302.

6. Gholizadeh, S. & Seyedpoor, S. M. (2011). Optimum design of arch dams for frequency limitations. *International Journal of Optimization in Civil Engineering*, Vol. 1, pp. 1-14.

7. Doǧan, E. & Saka, M. P. (2012). Optimum design of unbraced steel frames to LRFD−AISC using particle swarm optimization. *Advances in Engineering Software*, Vol. 46, pp. 27-34.

8. Kaveh, A. & Khayatazad, M. (2014). Optimal design of cantilever retaining walls using ray optimization method, *Iranian Journal of Science and Technology*, Vol. 38, No. C1$^+$, pp. 261- 274.

9. Kaveh, A., Talatahari, S. & Farhmand Azar, B. (2012). Optimum design of composite open channels using charged system search algorithm, *Iranian Journal of Science and Technology*, Vol. 36, pp. 67-77.

10. Kaveh, A. & Shokohi, F. (2014). Charged system search algorithm for the optimum cost design of reinforced concrete cantilever retaining walls, *Iranian Journal of Science and Technology*, Vol. 38, No. C1$^+$, pp. 235-249.

11. Kaveh, A. & Khayatazad, M. (2012). A new meta-heuristic method: ray optimization. *Computers and Structures*, Vol. 112-113, pp. 283–294.

12. Kaveh, A., Ilchi Ghazaan, M. & Bakhshpoori, T. (2013). An improved ray optimization algorithm for design of truss structures. *Periodica Polytechnica,* Vol. 57, No. 2, pp. 1-15.

13. Wang, D., Zhang, W. H. & Jiang, J. S. (2004). Truss optimization on shape and sizing with frequency constraints. *AIAA Journal*, Vol. 42, No. 3, pp. 622–630.

14. Lingyun, W., Mei, Z., Guangming, W. & Guang, M. (2005). Truss optimization on shape and sizing with frequency constraints based on genetic algorithm. *Computational Mechanics*, Vol. 25, No. 5, pp. 361–368.

15. Kaveh, A. & Zolghadr, A. (2012). Truss optimization with natural frequency constraints using a hybridized CSS-BBBC algorithm with trap recognition capability. *Computers and Structures*, Vol. 102-103, pp. 14-27.